GROWTH AND CHARACTERIZATIONS OF URINARY TYPE STRUVITE (MAGNESIUM AMMONIUM PHOSPHATE) CRYSTALS

R.Selvaraju and A.Sivasakthi

Department of Engineering Physics (FEAT), Annamalai University, Annamalai Nagar Tamilnadu, India

Department of Physics, Annamalai University, Annamalai Nagar, Tamilnadu,India

Abstract

Nephrolithiasis, also referred to as urolithiasis, is a pathological condition that causes urinary stones and is a major, incapacitating issue globally. Ammonium magnesium phosphate hexahydrate, or struvite- NH4MgPO4.6H20 is one of the constituents of urinary stones(calculi). Calcium, Ammonium and phosphate are the insoluble crystalline chemicals that make up urinary calculi. Urease-producing bacteria cause urinary tract infections, which lead to the development of struvite stones. The majority of urinary calculi issues in women are caused by struvite stones. The struvite crystals were grown using sodium metasilicate and ammonium dihydrogen phosphate as the growth medium. Here, we describe the single diffusion gel growth technique's kinetics of struvite in vitro crystallization. The analysis of FT-IR, Powder XRD and SEM-EDX were used to analyze the crystals. The orthorhombic crystal structure of struvite was validated by the powder XRD data. The existence of metal-oxygen bonds, P-O bond, N-H bonds and water of hydration was demonstrated by the FT-IR spectrum.

Key words; Struvite, Gel diffusion, XRD,

Introduction

Kidney stones are becoming more common place worldwide, mostly due to environmental factors and geographic location. Moreover, recognized risk factors for kidney stone disease are dietary practices, genetics, and lifestyle choices (Manzoor et.al., 2018; Das 2017). Kidney stones are a result of urine supersaturation, and solute concentration (Selvaraju & Bhuvaneswari 2020; Suryawanshi & Chaudhari 2014). The disorder known as urolithiasis is typified

by the development of stones in the bladder, Kidney, or urethra which cause discomfort. Struvite stones that result in kidney loss (Alelign & Petros 2018). The primary component of infections urinary stones, struvite, is linked to urolithic bacteria that cause chronic Urinary Tract Infections (UTIs) and make up 10-20% of all renal calculi (Polat & Eral 2022). Struvite is often called "urine sand ", Phosphatics tones, triple phosphate stones, infection stones or urease stones. Phosphate, Magnesium phosphate, Magnesium Hydrogen Phosphate Trihydrate, and Ammonium Magnesium Phosphate Hexahydrate ($NH_4MgPO_4.6H_2O$), are known to occur as components in urinary calculi in both men and women form adults to children. (Flannigan et.al., 2018; Schaffet & Pearson 2017; Karki & Leslie 2021) These stones have the potential to grow quickly and develop into staghorn-calculi, a more severe urological condition. These microbes divide urea into ammonium, which results in urine that is consistently alkaline ad then mixes with phosphate and magnesium (Bindhu et.al.,2015). Only struvite can cause difficulties such as pronephroses and form staghorn among all stone types. It can also harm the interior renal wall's epithelium, leading to kiney function loss (Prywer et.al., 2010). The single diffusion gel development approach offers a simpler in vitro representation of the intricate in vivo formation of urinary calculi. The struvite crystals that had developed were carefully extracted from the gel media. The gel growth technique involves the reaction of two solutions in a gel medium or the diffusion of a solution into a gel media to achieve super-saturation. Growing urinary crystals may be done most easily and adaptably with the gel approach (Chauhan & Joshi 2011; Selvaraju & Sulochana2017). In vitro crystallization , characterization and growth inhibition study of urinary type struvite cryslas.This communication report on the in vitro crystallization of struvite using the single diffusion gel growth approach in a silica hydrogel medium. The crystals were characterized using FT-IR spectroscopy, powder XRD and SEM-EDX method.

Materials and methods

AR-grade chemicals and distilled water were utilized to grow crystals. Struvite crystals were grown using the single diffusion gel growth process. Test tubes with diameters of 25 mm and length of 150 mm were used as a crystallization vessel. The gel medium was prepared using an aqueous solution of Sodium Meta Silicate (SMS) Na_2SiO_3. $9H_2O$ with a specific gravity of 1.03 gm/cm^{-3} and an aqueous solution of Ammonium Dihydrogen Phosphate (ADP) $NH_4H_2PO_4.2H_2O$ with a concentration of 0.5M. The SMS solution was combined with an aqueous solution of ADP (0.5M) in with a PH of 7.5 ensure that there are no air bubbles in the solution and the vessel is undisturbed. For appropriate gel setup, 20 ml of this solution was subsequently added to the crystallization vessels

respectively. Superior gels solidified in the test tube in two days. After gelation 0.5 M of Magnesium acetate was placed over the gel as a supernatant solution. The experiment was carried out at room temperature. It is anticipated that the two reactants, magnesium acetate as reactant -II in the supernatant solution (SS) and Ammonium Dihydrogen Phosphate (ADP) as reactant-I in the gel, would react as follows in the gel. The composition of the reactant (ADP) and the supernatant (Magnesium acetate) solutions are shown in the following Table 1. The struvite crystals that had developed were carefully extracted from the gel media. The growth and harvested of the struvite crystal is shown in fig 1a and 1b.

$$NH_4H_2PO_4.2H_2O + (CH_3COO)2Mg.4H_2O \longrightarrow NH_4MgPO_4.6H_2O + 2CH_3COOH$$

Table. 1. The optimum condition for the growth of struvite crystal

S.No	Parameters	Optimum Condition
1	Density of Sodium meta silicate	1.03 gm/cm^{-3}
2	PH of gel	7.5
3	Concentration $(MgCH_3COO)_2$	0.5 M
5	Concentration of $NH_4H_2PO_4$	0.5 M
6	Gel setting period	2 days
7	Gel aging	1 month
8	Period of growth	21 days
9	Temperature	Room Temperature

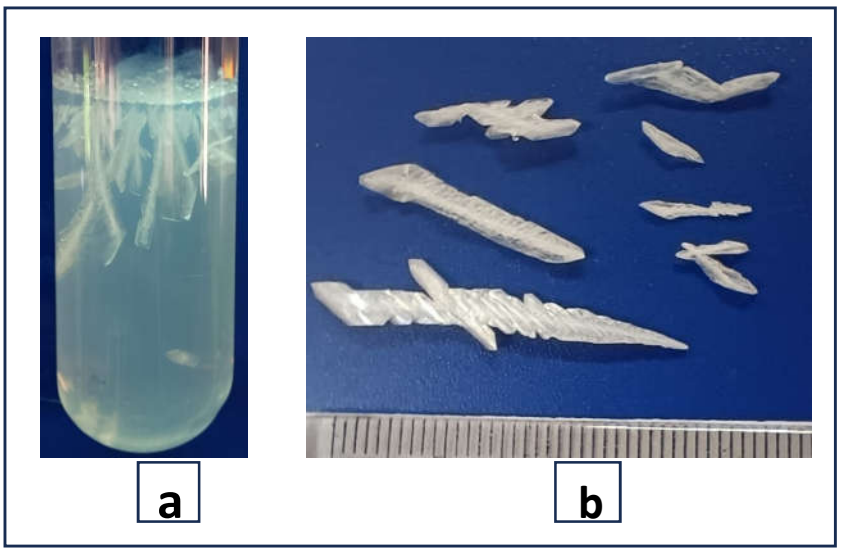

Fig 1 shows the growth and harvested of struvite crystals

Result and discussion

The struvite crystals are successfully grown by the single gel diffusion technique. FT-IR, XRD and SM with EDX are used to analyses the gel-grown crystals. In struvite crystals, the absorption peak at 1437 cm^{-1} is due to the presence of NH_4^+ (V_4) antisymmetric bending of ammonium. Phosphate and Metal oxygen bonds absorption peaks are identified by FT-IR analysis. The orthorhombic crystalline nature of struvite with increased peak intensity in (111), (002), (012) and (022) planes are observed with the help of XRD data. Further, the shape and morphology of the grown crystals are analysed by SEM. O, Mg and P are present in the struvite crystals. The atomic percentage and chemical composition are determined by SEM with EDX analysis (Ameen & Mohamed 2014; Muryanto et.al., 2016)

FT-IR spectra analysis

The grown struvite crystals FTIR spectrum, which was recorded between 400 and 4000 cm^{-1} is shown in Figure 2. The O-H and N-H stretching vibrations are responsible for a wide asymmetric band in the 3483,2931 cm^{-1} range (Bhagat & Popalghat 2014). The presence of metal-oxygen bonds, NH_4, PO_4^{3-}, N-H bonds and P-O bonds was confirmed by the FTIR spectra. The absorption detected at around 1645 cm^{-1} and 1437 cm^{-1} has been identified as the result of N-H bending vibrations. A strong band at 1007 cm^{-1} must originate from the components of the PO_4 vibration (Chauhan & Joshi 2013). Due to the O-H bonding to Mg $^{2+}$deforming, the phosphate PO_4^{3-}, peaks are absorbed at 891 cm^{-1} while a medium absorption band at 763 cm^{-1} indicates the wagging modes of vibration of the coordinated water. The peak at 568 cm^{-1} is due to the asymmetric bending modes of the PO_4 units and the peak 462 at metal-oxygen bond. A summary of the vibrational band assignments and observed wave numbers is provided in Table 2. Thus, FTIR spectroscopy confirmed the growth of struvite crystals was due to the presence of water molecules, stretching and bending vibrations of phosphate (PO_4) ions and Mg-O bond. The FTIR pattern of the gel-grown struvite crystals matches the values published in the literature.(Bindhu &Thambi 2012; Vasuki & Selvaraju 2019).

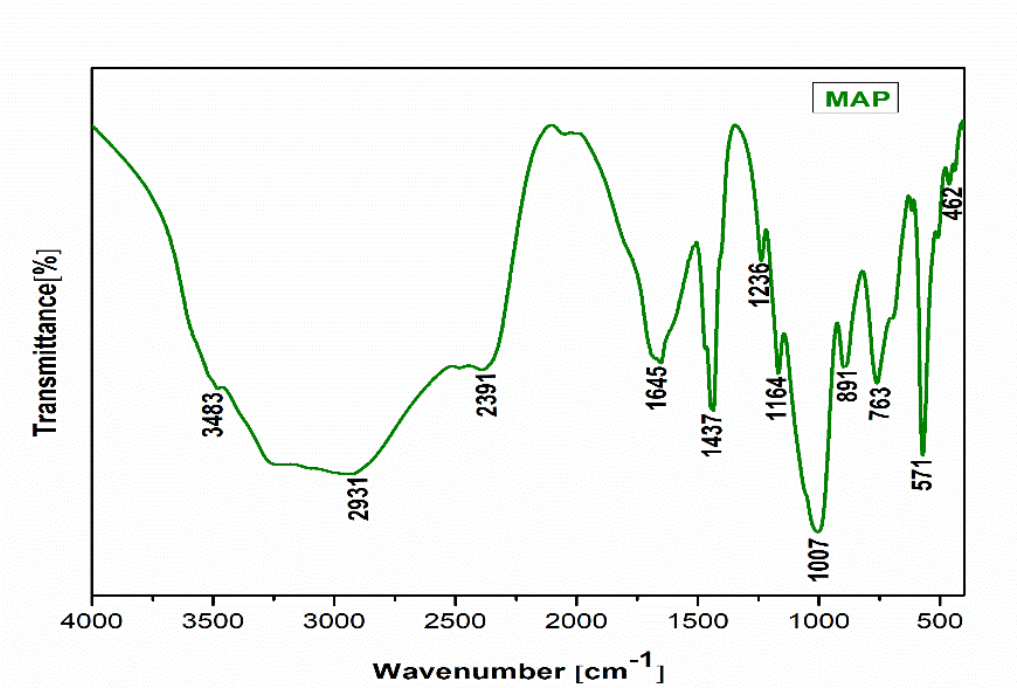

Fig .2 FT-IR spectrum of struvite crystal

Table. 2. Vibrational band assignments of grown crystals

Pure struvite Wavenumber (cm^{-1})	Vibration band Assignment
3483	O-H stretching vibration
2931	NH^{+}_4 Symmetric stretching
2371	H-O-H stretching
1645	NH^{+}_4 Symmetric bending
1437	NH^{+}_4 Asymmetric bending
1236	PO_4^{3-}Asymmetric stretching
1164	PO_4^{3-}Asymmetric stretching
1007	PO_4^{3-}Asymmetric stretching
891	PO_4^{3-} Symmetric stretching deformation of OH linked to Mg^{2+}
763	Wagging modes of vibration of coordinated water
571	PO_4^{3-} Asymmetric bending
462	Metal-oxygen bond

XRD analysis

Powder XRD is used to assess the Crystallinity, structure and phase of the struvite crystals that the generated in vitro. Utilizing CuKα radiation at 1.5406 Å wavelength, the investigation is carried out with a Philips Xpert diffractometer. The findings validate the material crystalline structure and phase purity (Figure 3). Based on the XRD pattern, the formed crystals' hkl values,d spacing and lattice parameters are determined. The crystals exhibit an orthorhombic crystalline structure. Struvite crystallization is caused by the strong peaks at (111), (002), (012) and (022) planes with high intensity, which matches well with JCPDS No: (77-2303). The diffraction peaks were all clearly identified as struvite, with no signs of other impurity phases. The outcomes aligned with previous research findings (Chauhan & Joshi 2013; Bindhu et.al., 2015)

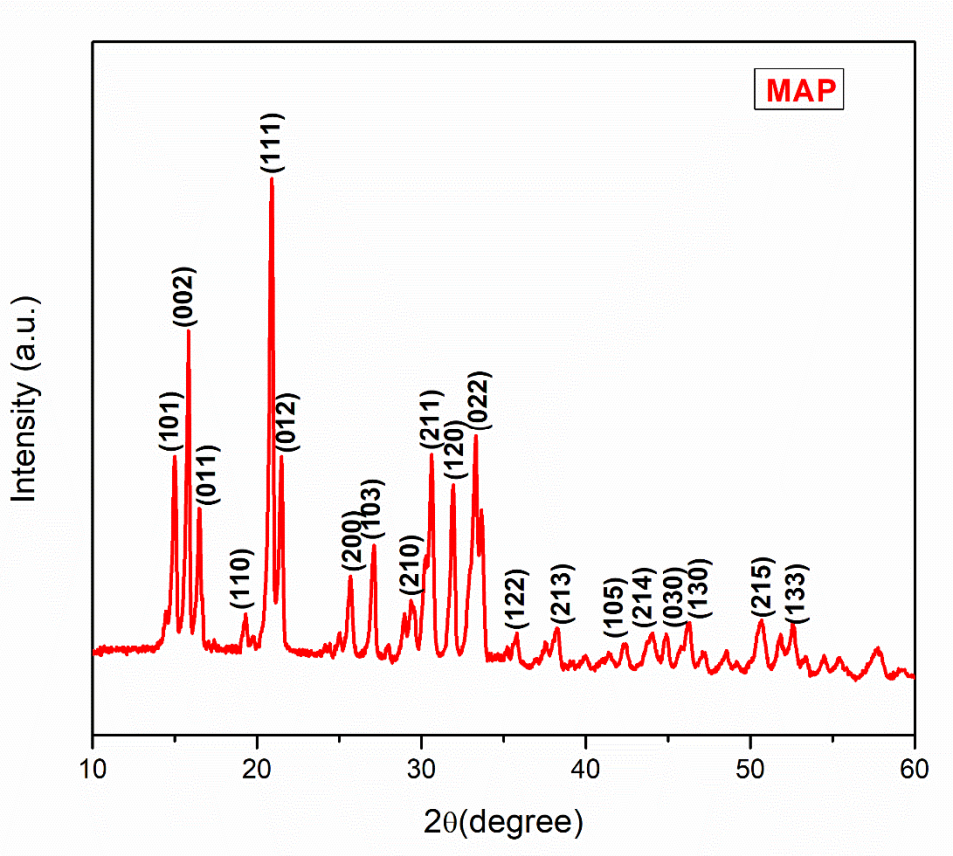

Fig .3 XRD spectrum of struvite crystal

Table. 3. XRD data for Pure Struvite crystals

Observed value			Standard value			h k l
2θ	**I/I_o**	**d-spacing (Å)**	**2θ**	**I/I_o**	**d-spacing (Å)**	
14.86	42	5.96	14.97	38	5.91	**101**
15.76	80	5.62	15.78	60	5.60	**002**
16.47	37	5.39	16.44	24	5.38	**011**
19.01	10	4.69	19.26	4	4.60	**110**
20.75	100	4.28	20.84	100	4.25	**111**
21.41	50	4.16	21.43	34	4.14	**012**
25.66	24	3.47	25.59	9	3.47	**200**
27.02	33	3.29	27.05	24	3.29	**103**
29.24	11	3.05	29.49	10	3.02	**210**
30.48	56	2.93	30.57	44	2.92	**211**
31.84	46	2.81	31.88	28	2.80	**120**
33.39	60	2.68	33.23	40	2.69	**002**
35.73	8	2.51	35.71	5.6	2.51	**122**
38.20	12	2.35	38.23	9	2.35	**213**
42.37	8	2.13	42.41	5	2.12	**222**
43.98	10	2.05	43.98	8	2.05	**214**
44.04	10	2.03	44.20	2	2.04	**030**
46.14	14	1.96	46.18	4	1.96	**130**
50.69	17	1.80	50.60	9	1.80	**215**
52.60	15	1.73	52.59	11	1.73	**133**

SEM-EDX analysis

The struvite crystals morphological characteristics were examined by the use of scanning electron microscopy (SEM). Energy dispersive X-ray analysis is used to determine the material's elemental composition. Figure 4 displays the EDS spectra of the struvite sample. The crystal morphology is spherical-shaped. (Manzoor et.al.,2019). Table 4 shows the atomic percentage of struvite for O, Mg, and P is 57.02%,16.93% and 26.04% respectively (Suguna et.al., 2012).

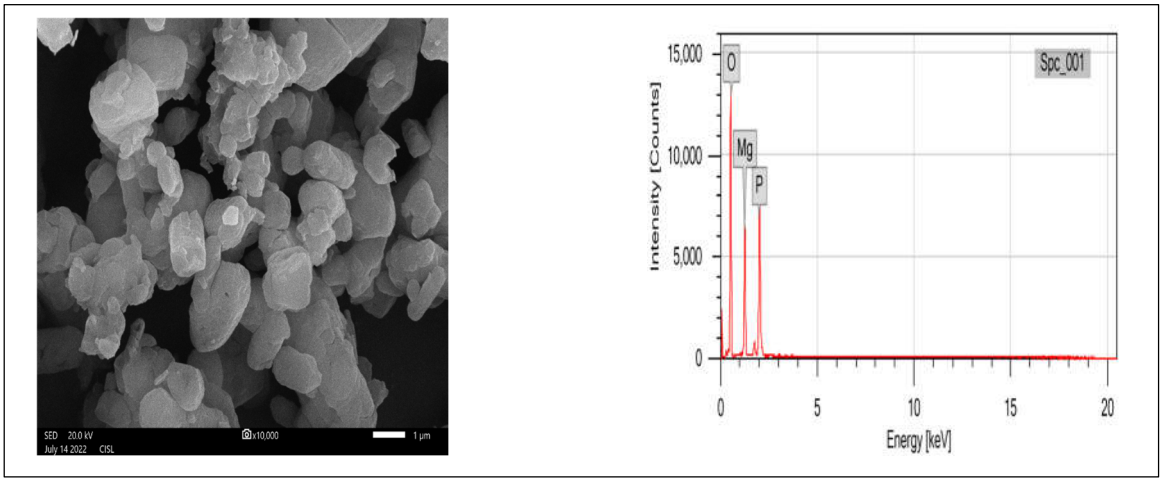

Fig.4 SEM and EDX spectrum of struvite crystal

Table 4 shows the elemental composition and atomic percentage of struvite crystals

Elements	Mass %
O	57.02
Mg	16.93
P	26.04

Conclusion

Struvite crystals are successfully grown and harvested using a single gel diffusion method. The grown crystals are assessed with spectroscopic techniques such as FTIR, XRD, and SEM with EDX. The chemical composition in the struvite crystals is identified and it shows strong ammonium, phosphate and magnesium peaks which confirms the crystallization of magnesium ammonium phosphate. The struvite is crystallized in orthorhombic structure XDR. The struvite crystal EDX spectrum shows the presence of O, Mg and P. The crystal morphology is Spherical-shaped. The crystallization techniques are revisited and confirm the crystallization process. The invitro crystallization is used to understand the nucleation, aggregation and growth of the struvite

Reference

1. Alelign, T., & Petros, B. (2018). Kidney stone disease: an update on current concepts. *Advances in urology*, *2018*(1), 3068365.

2. AMEEN, S. M., & MOHAMED, A. S. ASIAN ACADEMIC RESEARCH JOURNAL OF MULTIDISCIPLINARY.
3. Bhagat, A. C., & Popalghat, S. K. (2014). The Study of Crystal Growth of Struvite in Gel Media. *Deccan Current Science Research Journal*, *9*(11), 283-286.
4. Bindhu, B., & Thambi, T. A. (2012). Formation and microanalysis of struvite urinary calculi. *International Journal of Engineering Research and Applications*, *2*, 1480-1485.
5. Bindhu, B., Swetha, A. S., & Veluraja, K. (2015). Studies on the effect of phyllanthus emblica extract on the growth of urinary type struvite crystals invitro. *Clinical Phytoscience*, *1*, 1-7.
6. Chauhan, C. K., & Joshi, M. J. (2013). In vitro crystallization, characterization and growth-inhibition study of urinary type struvite crystals. *Journal of Crystal Growth*, *362*, 330-337.
7. Das, P., Gupta, G., Velu, V., Awasthi, R., Dua, K., & Malipeddi, H. (2017). Formation of struvite urinary stones and approaches towards the inhibition—A review. *Biomedicine & Pharmacotherapy*, *96*, 361-370.
8. Flannigan, R. K., Battison, A., De, S., Humphreys, M. R., Bader, M., Lellig, E., ... & Lange, D. (2018). Evaluating factors that dictate struvite stone composition: a multi-institutional clinical experience from the EDGE Research Consortium. *Canadian Urological Association Journal*, *12*(4), 131.
9. Karki, N., & Leslie, S. W. (2021). Struvite and Triple Phosphate Renal Calculi.
10. Manzoor, M. A., Mujeeburahiman, M., Duwal, S. R., & Rekha, P. D. (2019). Investigation on growth and morphology of in vitro generated struvite crystals. *Biocatalysis and Agricultural Biotechnology*, *17*, 566-570.
11. Manzoor, M. A., Singh, B., Agrawal, A. K., Arun, A. B., Mujeeburahiman, M., & Rekha, P. D. (2018). Morphological and micro-tomographic study on evolution of struvite in synthetic urine infected with bacteria and investigation of its pathological biomineralization. *PLoS One*, *13*(8), e0202306.
12. Muryanto, S., Sutanti, S., & Kasmiyatun, M. (2016). Inhibition of struvite crystal growth in the presence of herbal extract orthosiphon aristatus BL. MIQ. In *MATEC web of conferences* (Vol. 58, p. 01013). EDP Sciences.
13. Polat, S., & Eral, H. B. (2022). Effect of hyaluronic acid on the struvite crystallization: A structural, morphological, and thermal analysis study. *Journal of Crystal Growth*, *592*, 126734.

14. Prywer, J., & Torzewska, A. (2010). Biomineralization of struvite crystals by Proteus mirabilis from artificial urine and their mesoscopic structure. *Crystal Research and Technology*, *45*(12), 1283-1289.
15. Schaffer, J. N., & Pearson, M. M. (2017). Proteus mirabilis and urinary tract infections. *Urinary tract infections: Molecular pathogenesis and clinical management*, 383-433.
16. Selvaraju, R., & Sulochana, S. (2016). In-vitro growth and inhibition studies of Tribulus terrestris on calcium oxalate monohydrate crystals. *International Journal of Science and Research*, *5*(6), 83-87
17. Suryawanshi, V. B., & Chaudhari, R. T. (2014). Synthesis and characterization of struvite-k crystals by agar gel. *Journal of Crystallization Process and Technology*, *4*(04), 212.